scientific reports

Check for updates

OPEN

Stratification of G2 pancreatic neuroendocrine tumors using a Ten Percent Ki-67 index cut-off based on clinicopathological and molecular analyses

Yumiko Kageyama[1], Ryo Ashida[1]✉, Nobuyuki Ohike[2,3], Keiichi Ohshima[4], Tomoko Norose[2,3], Katsuhisa Ohgi[1], Mihoko Yamada[1], Shimpei Otsuka[1], Yoshiyasu Kato[1], Hidemasa Kubo[1], Katsuhiko Uesaka[1], Teiichi Sugiura[1], Takashi Sugino[2], Akihumi Notsu[5], Akane Naruoka[6], Takeshi Nagashima[7,8], Kenichi Urakami[7] & Ken Yamaguchi[9]

Pancreatic neuroendocrine tumors (PanNETs) often have low malignancy, but some develop distant metastasis or recurrence. This study aimed to investigate the prognostic utility of a Ki-67 index 10% cut-off using clinicopathological and multiomics analyses. Eighty-seven resected PanNETs were classified as G1, G2-low, G2-high, and G3 according to the World Health Organization classification, incorporating a 10% Ki-67 threshold. These groups comprised 29 (33%), 33 (38%), 16 (18%), and 9 (10%) patients, respectively. Comprehensive analyses evaluated tumor characteristics and mutation profiles across the groups. Significant differences in tumor size, recurrence, and overall survival were observed between the G2-low and G2-high groups. Genomic profiling of 19 samples revealed that the G3 (4 patients) and G2-high (6 patients) groups showed greater tumor mutation burdens and more driver gene mutations than the G2-low (6 patients) and G1 (3 patients) groups. Gene expression profiling revealed distinct patterns between the G3/G2-high and G2-low/G1 groups, with the oncogene *SERPINA1* significantly upregulated in the G3/G2-high group. The multiomics approach identified key genes, emphasizing the significance of the Ki-67 index 10% cut-off in predicting tumor behavior. The findings support using the Ki-67 index of 10% as a critical threshold for stratifying PanNETs and guiding prognosis and treatment.

Keywords Gene mutations, Ki-67 index, Molecular genetics, Pancreatic neuroendocrine tumors, Whole-exome sequencing

Pancreatic neuroendocrine tumors (PanNETs) are considered to have relatively low malignancy. This is especially true for NET G1/G2, which are sometimes considered low-risk. However, cases of distant metastasis or recurrence have been reported[1,2].

A number of reports have stated that the classification of PanNETs using Ki-67 index cut-off values other than those specified in the World Health Organization (WHO) classification (3% and 20%) may more accurately predict prognosis[3–5]. Several previous reports have shown that a Ki-67 index cut-off of 10% is useful for the prognostication of PanNETs[3,4]. Furthermore, the European Society for Medical Oncology (ESMO) Clinical Practice Guidelines have proposed a treatment algorithm with a Ki-67 index cut-off of 10%[6]. For the surgical treatment of well-differentiated PanNETs (NET G1/G2) with distant metastases, a Ki-67 index of < 10% is among

[1]Division of Hepato- Biliary-Pancreatic Surgery, Shizuoka Cancer Center, 1007 Shimonagakubo, Nagaizumi-cho, Sunto-gun, Shizuoka 411-8777, Japan. [2]Division of Pathology, Shizuoka Cancer Center, Shizuoka, Japan. [3]Division of Molecular Pathology, Department of Pathology, St. Marianna University School of Medicine, Kawasaki, Japan. [4]Medical Genetics Division, Shizuoka Cancer Center Research Institute, Shizuoka, Japan. [5]Clinical Research Center, Shizuoka Cancer Center, Shizuoka, Japan. [6]Drug Discovery and Development Division, Shizuoka Cancer Center Research Institute, Shizuoka, Japan. [7]Cancer Diagnostics Research Division, Shizuoka Cancer Center Research Institute, Shizuoka, Japan. [8]SRL, Inc., Tokyo, Japan. [9]Shizuoka Cancer Center Hospital and Research Institute, Shizuoka, Japan. ✉email: r.ashida@scchr.jp

the requirements. For multidisciplinary treatment, somatostatin analogs constitute the first-line treatment for NET G2 with Ki-67 indexes of < 10%, as in NET G1.

In the present study, we focused on the differences in gene mutations and their expressions to verify the usefulness of adding a Ki-67 index of 10% as a cut-off value for grading. We also tested whether a 10% cut-off for resected PanNETs would have an impact on prognosis. The PanNETs were first classified into three groups according to the WHO classification and based on the Ki-67 indices (< 3% as G1, 3–20% as G2, and > 20% as G3). G2 was subsequently further divided into G2-high and G2-low based on the Ki-67 index cut-off of 10%. The characteristics of the four groups were explored using clinicopathological studies and comprehensive analyses, including immunohistochemical evaluations, whole exome sequencing (WES), deep sequencing of a comprehensive cancer panel (CCP), and gene expression profiling (GEP) to validate the classification.

Materials and methods

Patient selection

In this retrospective observational study, 87 Japanese patients who underwent surgical resection (R0 or R1) for PanNETs between 2005 and 2022 at the Shizuoka Cancer Center Hospital were included. All resected specimens were reviewed in this study. The exclusion criteria were histologically proven mixed neuroendocrine-non-neuroendocrine neoplasm or cases in which non-curative surgery was performed. The clinical data of the patients were retrieved from a prospectively maintained database. The need for patient consent was waived by the Institutional Review Board of the Shizuoka Cancer Center because of the retrospective nature of this study. Approval was obtained from the Institutional Review Board of the Shizuoka Cancer Center (approval number J2022-198–2022-1–2) before data collection.

Since 2014, we have been conducting a cancer multiomics study called Project HOPE (High-tech Omics-based Patient Evaluation), which aims to establish established the Japanese version of The Cancer Genome Atlas[7]. From 2014 to 2022, a total of 62 cases of PanNET were resected, of which 20 were analyzed as part of the Project HOPE. In this study, 19 cases were included except for one case in which specimen contamination was suspected. Consent was also obtained from all patients who underwent the multiomics analysis. All experiments using clinical samples were carried out following approved guidelines. Ethical approval for all experimental protocols and studies was obtained from the Institutional Review Board of the Shizuoka Cancer Center (Authorization Numbers: 25–33).

Treatment strategies and follow-up

Pancreatectomy with regional lymph node dissection was performed for patients with histologically diagnosed or strongly suspected PanNETs based on imaging studies with regional lymph node dissection. For small tumors, less extensive surgery has been considered[8]. For resectable synchronous liver metastases, simultaneous hepatectomy was performed. None of the patients received any neoadjuvant or postoperative adjuvant therapy. Patients were followed up every 3 months to 1 year after surgery, depending on the grade of their PanNET and their general condition. Recurrence was diagnosed according to radiologic or histologic findings.

Clinicopathological characteristics

Patient demographics, resection type, tumor size, tumor functionality, tumor heredity, TNM classification, recurrence, survival status, and date were extracted from the patient records. The tumor size was measured using the resected specimen. Histopathological diagnoses were assessed by at least two pathologists (NO and TN). MEN1 was diagnosed based on the following: two lesions in three major organs or one lesion and a family history of *MEN1* mutation[9]. The UICC 8 th edition was referenced for staging[10].

Immunohistochemical evaluation

Immunohistochemical staining was performed using the Leica Bond-III automated immunostainer (Leica Biosystems, Melbourne Pty. Ltd., Australia) to ensure standardized and reproducible results. Tissue sections were dewaxed with Bond Dewax Solution and subjected to heat-induced epitope retrieval using Bond Epitope Retrieval Solution (ER1 or ER2), depending on the specific antibody requirements. Endogenous peroxidase activity was blocked, followed by incubation with primary antibodies at the recommended dilutions and durations. Detection was carried out using the Bond Polymer Refine Detection Kit (DS9800), and chromogenic development was used to visualize antigen–antibody complexes. Hematoxylin counterstaining was performed to enhance tissue contrast, and the sections were dehydrated, cleared, and mounted for microscopic evaluation. Quality control measures included the use of appropriate positive and negative controls to confirm staining specificity and reliability.

Ki-67 immunostaining was conducted using the MIB1 antibody (dilution 1:100; Agilent Technologies) to assess tumor proliferative activity. The Ki-67 index was determined by manually counting at least 500 tumor cells within hotspot areas where Ki-67-positive nuclei were most densely distributed, based on color-printed photographic images[11]. According to the WHO classification, 87 patients were categorized into G1, G2, and G3 based on their Ki-67 index. Additionally, G2 was further subdivided into G2-low and G2-high using a 10% Ki-67 index as the cutoff. The clinical utility of this four-tiered grading system was subsequently evaluated.

Somatostatin receptor 2 (SSTR2) expression was assessed using the Volante scoring system[12] with the prediluted EP149 antibody (Nichirei Bioscience). Membranous immunoreactivity corresponding to a Volante score of 2 or 3 was considered SSTR2-positive. To confirm the results of genetic analyses, additional immunohistochemical staining was performed for DAXX (clone E94, dilution 1:100; Abcam) and ATRX (clone 23 C, dilution 1:1000; Sigma-Aldrich).

Analysis of somatic mutations, germline variants and gene expression profile

We performed WES and deep sequencing of CCP using blood samples collected during surgery and fresh surgical samples obtained after surgery in Project HOPE[7]. Tumor and matched normal samples were collected. Measurements of WES/CCP and GEP were performed using the Ion Proton system and Agilent system. Experimental procedures are described in detail in previous reports[7,13]. The mean depth of coverage of the target regions was 134.9-fold for WES and 1173.7-fold for CCP. Mutations classified under tier 1 were defined as driver mutations. Mutations classified under tier 2 were defined as likely driver mutations. A smaller tier number represents a higher confidence level of supporting data. Nonsense, frameshift, and splice acceptor/donor site mutations were considered as truncating mutations. Oncogene mutations satisfying all of the following criteria were classified as tier 3: (1) noncommon SNPs, (2) CADD score of ≥ 20 or predicted as pathogenic by FATHMM, (3) observed in ≥ 5 samples in the HOPE cohort. Variants of uncertain significance (VUS) were classified as tier 4. Somatic CNVs were detected using saasCNV. This method accounted for both the read-depth ratio and B allele frequency and achieved the best performance among six CNV detection tools. CNV increase of 4 or more or decrease of less than 1 was considered significant. The microsatellite instability (MSI) status was determined using MSIsensor from standard tumor-normal paired sequence data[14]. We also conducted GEP of matched tumors and adjacent normal tissues from each patient using an Agilent DNA microarray system[15]. The GEP change was considered significant with a fold change of 5 or more or a decrease of − 5 or less.

Quantitative RT-PCR analysis

Quantitative mRNA levels were determined using real-time RT-PCR using the Applied Biosystems 7900 HT Sequence Detection System, TaqMan Gene Expression Assays for the oncogenes and tumor suppressor genes (TSGs) classified by clustering of microarray expression data (Supplementary Data 1), and a Eukaryotic 18 S rRNA Endogenous Control (Applied Biosystems; Thermo Fisher Scientific, Inc.). cDNA was generated using 100 ng of total RNA, and a High Capacity cDNA Reverse Transcription Kit (Applied Biosystems; Thermo Fisher Scientific, Inc.). RT-PCR was carried out in a total volume of 20 µl containing 100 ng of cDNA, TaqMan Fast Advanced Master Mix (Applied Biosystems), and the respective TaqMan target gene reagents. The amplification conditions were 95 °C for 20 s followed by 40 cycles of 95 °C for 1 s and 60 °C for 20 s. Samples were analyzed in triplicate as technical replicates. The mRNA levels were defined from the cycle threshold (Ct), using the comparative Ct method[16], and normalized by comparison to 18 S rRNA levels. This value was expressed as ΔCt, with lower values indicating higher expression.

Statistical analysis

Categorical variables are presented as frequencies with percentages and compared by the chi-squared or Fisher's exact test. Continuous variables are expressed as medians and ranges and compared using the Mann–Whitney U test. Correlation was measured with the Spearman's rank correlation coefficient. Overall survival (OS) was defined as the date of resection to the date of death from any cause. Patients who were alive at the date of the last follow-up were censored at that date. Recurrence-free survival (RFS) was calculated from the date of resection to the date of disease recurrence or death from any cause. Patients without recurrence at the date of the last follow-up were censored at that date. The Kaplan-Meier method was used to estimate survival, and the log-rank test was used to compare the survival curves of the two groups. The Cox proportional hazards model was used to assess independent risk factors and estimate hazard ratios for DFS. The statistical analyses were performed using EZR (Saitama Medical Center, Jichi Medical School), which is a graphical user interface for R (R Foundation for Statistical Computing). Student's *t*-test for comparison of ΔCt values was used. P-values < 0.05 were considered to indicate a statistically significant difference.

Results

Clinicopathological and immunohistochemical data

The median age was 64 years (range, 36–86 years), and 44 of the 87 patients were male (51%). Distal pancreatectomy, pancreatoduodenectomy, and central pancreatectomy were performed for 41 (47%), 30 (34%), and 13 (15%) cases, respectively. Total pancreatectomy and enucleation were also performed. Concomitant hepatectomy for liver metastases was performed for 7 (8%) cases. Functional tumors were observed in one patient (1%); it was an insulinoma. MEN1 comorbidity was observed in five cases (6%). The median follow-up duration was 61 months (range: 2–179 months). SSTR2 was positive for 82 cases (94%), and the positivity rates were high even with high Ki-67 index values.

Patient characteristics and survival related to the Ki-67 index

Table 1 shows the comparison of the clinicopathological and immunohistochemical findings of the 87 patients divided into four groups. Twenty-nine (33%), 33 (38%), 16 (18%), and 9 (10%) cases were classified as G1, G2-low, G2-high, and G3, respectively. Synchronous liver metastases were found in 1 patient with G2-low (3%), 2 with G2-high (13%), and 4 with G3 (44%). Recurrence was observed in 1 patient with G2-low (3%), 5 with G2-high (31%), and 6 with G3 (67%). The lesions were localized in the liver in 11 cases and in the bone in 2 cases (including 1 duplicate). Significant differences were found between G2-low and G2-high in tumor diameters (20 mm vs. 39 mm, $p = 0.013$), perineural invasion (9% vs. 44%, $p = 0.008$), and recurrence rate (3% vs. 31%, $p = 0.011$), as well as in vascular invasion between G1 and G2-low (7% vs. 33%, $p = 0.013$). Tumor size, distant metastasis, vascular invasion, and perineural invasion correlated with the four-group classification (Fig. 1). Multivariate Cox regression survival analysis revealed that only the four-group classification was independently associated with poor RFS (Supplementary Data 2). Figure 2 shows the results of Kaplan-Meier survival analysis stratified into four groups. The 5-year OS rates were 100% for G1, 96% for G2-low, 88% for G2-high, and 75% for

Grade Ki-67 index		G1 < 3%	G2-low 3–10%	G2-high 10–20%	G3 20%<	*p*		
						G1 vs. G2-low	G2-low vs. G2-high	G2-high vs. G3
n		29 (33%)	33 (38%)	16 (18%)	9 (10%)			
Age*		65 (36–79)	62 (40–85)	68 (46–86)	61 (40–75)	0.459	0.245	0.126
Sex, Male		16 (55%)	13 (39%)	9 (56%)	6 (67%)	0.308	0.361	0.691
Location	Head	11	14	6	5			
	Body-tail	21	19	10	4			
Tumor size, mm*		13 (4–70)	20 (8–45)	39 (7–145)	35 (22–48)	0.066	0.013	0.712
Lymph node metastasis (+)		3 (10%)	7 (21%)	3 (19%)	4 (44%)	0.312	1.000	0.205
Distant metastasis (+)		0 (0%)	1 (3%)	2 (13%)	4 (44%)	1.000	0.245	0.142
Vascular invasion (+)		2 (7%)	11 (33%)	10 (63%)	9 (100%)	0.013	0.070	0.057
Perineural invasion (+)		2 (7%)	3 (9%)	7 (44%)	5 (50%)	1.000	0.008	0.688
Symptomatic (Insulinoma)		1 (3%)	0 (0%)	0 (0%)	0 (0%)	0.301	n.a.	n.a.
Hereditary (MEN1)		2 (7%)	3 (9%)	0 (0%)	0 (0%)	1.000	0.541	n.a.
Ki-67 index*		1.8 (0.3–2.8)	4.8 (3.3–9.8)	11.9 (10.0–18.4)	20.3 (20.3–44.6)			
SSTR2 (+)†		27 (93%)	31 (94%)	16 (100%)	8 (89%)	0.432	0.158	0.120
Recurrence		0 (0%)	1 (3%)	5 (31%)	6 (67%)	1.000	0.011	0.115
	-Liver	0	1	5	5			
	-Bone	0	0	1	1			
Death due to NET		0 (0%)	1 (3%)	2 (13%)	3 (33%)	1.000	0.245	0.312

Table 1. Clinicopathological and immunohistochemical findings of the four groups. * Median. † IHC, Volante scores of 2–3.

G3 cases. The 5-year RFS rates were 100%, 97%, 66%, and 0%, respectively. The differences between the G2-low and high groups were significant for both OS ($p = 0.045$) and RFS ($p = 0.004$).

Somatic mutations and germline variants

Figure 3 shows the oncoprint of WES and CCP, demonstrating the distribution of somatic and germline variants in 19 cases of PanNETs for 1988 cancer-related genes[17] (Supplementary Data 3–6). The number of mutations was significantly higher for the groups with Ki-67 indices of ≥10% (G3 and G2-high) than for those with Ki-67 indices of <10% (G2-low and G1) (median number; 2 vs. 0, $p = 0.036$). Among the chromatin remodeling genes, truncating mutations in *DAXX* and *ARID1 A* were observed in two G2-high cases (Cases 8 and 10) and one G2-low case (Case 13), respectively. The patient with G2-high (Case 7) harbored a VUS mutation in *ATRX*. Immunostaining of the tumor tissues with these *DAXX* truncating mutations (Cases 8 and 10) and a VUS mutation in *ATRX* (Case 7) showed loss of expression of the respective proteins (Fig. 4). Regarding genes associated with PanNET, mutations were also found in G2-high for *PTEN* (Case 7), *TSC1* (Case 7), *MEN1* (Cases 6 and 9), *SETD2* (Case 9), and *KMT2D* (Cases 6 and 9). In addition, a *SETD2* mutation was found in one case of G2-low (Case 13), and *VHL* mutations were found in two cases of G3 (Cases 2 and 4). Recurrence was observed for six cases, including three cases of G3 (Cases 1, 2, and 3) and three cases of G2-high (Cases 6, 7, and 8). Two deaths were recorded, and both were G3 cases (Cases 1 and 2). One of the three G2-high cases with recurrence had truncating mutations in *MEN1* and *TP53* (Case 6). The other two cases had truncating mutations in *PTEN* and *TSC1*, a VUS mutation in *ATRX* (Case 7), and a truncating mutation in *DAXX* (Case 8). Germline mutations were found in two G2-high cases; *BAP1*, *CASQ2*, and *TSC2* mutations were observed for Case 9, and a *MSH3* mutation was observed for Case 10.

Comprehensive gene expression analysis

PanNET genes were roughly divided into three clusters based on GEP analyses (Fig. 5). Due to inadequate specimens, a comprehensive gene expression analysis was performed for 17 cases. The genes in each cluster are listed in Table 2. Cluster 1 contained genes upregulated in the groups with Ki-67 indices of ≥10% (G3 and G2-high). They included 4 oncogenes (*BIRC5*, *CDH12*, *ELANE*, and *SERPINA1*). On the contrary, cluster 2 contained genes upregulated in the groups with Ki-67 indices of <10% (G2-low and G1). They included 2 oncogenes (*ANK1 and FOXQ1*) and 2 tumor suppressor genes (TSG) (*AZGP1* and *MSMB)*. Cluster 3 contained genes that were downregulated mainly in the groups with Ki-67 indices of ≥10% (G3 and G2-high) and upregulated in some of the groups with Ki-67 indices of <10% (G2-low and G1). They included *DTX1*, one of the TSGs, and 7 genes showing expressions in normal pancreatic islets (*CEL*, *CLPS*, *CPA1*, *CPA2*, *PLA2G1B*, *PNLIP*, and *PNLIPRP2*).

The expression levels of seven oncogene or TSGs that showed expression changes in each cluster were validated by RT-PCR (Fig. 6). Among these, *SERPINA1* was the only oncogene with a significantly altered expression, showing increased levels in samples with Ki-67 indices ≥10% (G3 and G2-high) compared to those with Ki-67 indices <10% (G2-low and G1). The other six genes exhibited trends of either increased or decreased expression, but no statistically significant differences were observed between the two groups.

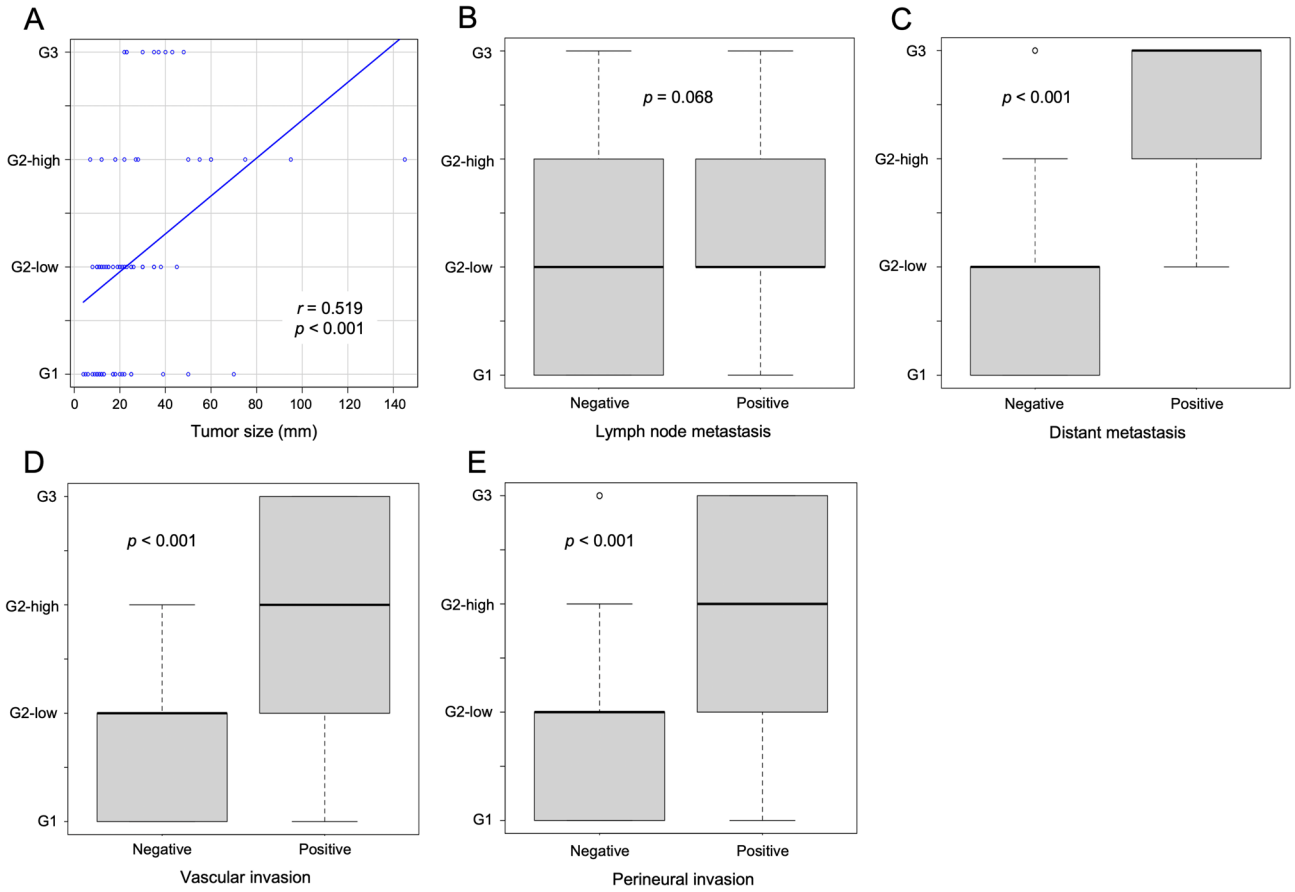

Fig. 1. Associations between four-group classification and tumor size **(A)**, lymph node metastasis **(B)**, distant metastasis **(C)**, vascular invasion **(D)**, perineural invasion **(E)**. Tumor size, distant metastasis, vascular invasion, perineural invasion correlated with the four-group classification ($p < 0.001$).

Discussion

Various studies have investigated predictive factors for the prognosis and treatment response in PanNETs. The analysis using WES and CCP presented here further elucidates the molecular underpinnings of PanNETs in relation to the Ki-67 index stratification. In this study, more genetic mutations were found in the groups with Ki-67 indices of ≥ 10%. Comprehensive gene expression analysis showed that the cluster containing oncogenes tended to be upregulated in the groups with Ki-67 indices of ≥ 10%, while the cluster containing TSG and genes expression in normal pancreatic islets tended to be upregulated in the groups with Ki-67 indices of < 10%. This may indicate that PanNETs have different biological grades with a Ki-67 index of 10% as a boundary, and the results suggests that the use of a Ki-67 index of 10% as a cut-off for classification may improve prognosis prediction.

Somatic mutations in PanNETs are well characterized; for example, *MEN1*, *DAXX*, *ATRX*, and *PTEN* have been identified as driver genes[18–20]. *MEN1* is a component of a histone methyltransferase complex and functions as a transcriptional regulator[21], while *DAXX* and *ATRX* are involved in telomere maintenance through the alternative lengthening of the telomere (ALT) pathway[22]. Furthermore, *PTEN* and *TSC1*, which are mTOR pathway-related genes involved in tumor cell growth, have been associated with poor prognoses[19,23]. These genes were mutated in G2-high cases in our study, which may be related to the poor prognosis of G2-high cases.

With regard to differences in genomic abnormalities stratified by the PanNET grade, Yachida et al. reported that *TP53* mutations and *CDKN2 A* hypermethylation were observed in some cases of G3, but rarely in cases of G1 and G2[24]. In the present study, *TP53* mutations were found in G2-high, which may also be related to the poor prognosis of G2-high cases. Furthermore, *VHL* gene mutations observed in G3 in the present study have been reported to cause renal cancer by preventing the degradation of hypoxia-inducible factors. This may be related to the similarity of PanNETs and renal cancer to hypervascular tumors[25]. Further analysis of genetic variations in PanNETs may reveal new genetic variants involved in the development of PanNETs and may help elucidate their development and high-grade malignant transformation.

Cluster analysis revealed the following. Cluster 1 included the following oncogenes. *BIRC5* is an immune-related gene that inhibits apoptosis and promotes cell proliferation, and it is a target for molecular imaging and the detection of pancreatic cancer[26,27]. *CDH12* is a subtype of the N-cadherin family that increases the proliferation and migration of cancer cells. It is also involved in the progression of lung, salivary gland-like cystic, and colorectal cancer[28]. *SERPINA1* is a serpin peptidase inhibitor that regulates the invasive and metastatic potential of lung,

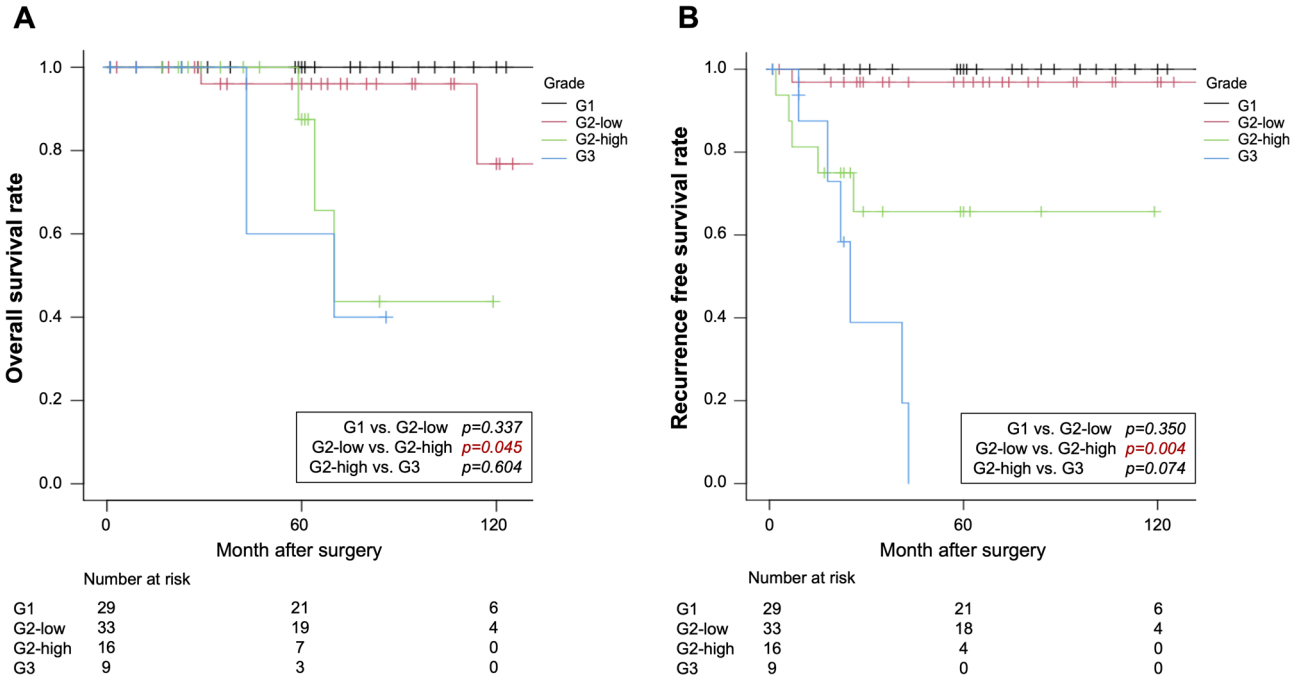

Fig. 2. Kaplan-Meier survival curves of pancreatic neuroendocrine tumors. Overall survival **(A)** and recurrence-free survival **(B)** of patients subdivided into four groups (G1, G2-low, G2-high, and G3) with Ki-67 indices of 3%, 10%, and 20% as the cutoff values. The differences between the G2-low and high groups were significant for both overall survival and recurrence-free survival ($p = 0.004$).

gastric, and colorectal cancers[29]. These genes may be associated with higher malignancy of high-grade PanNETs. Cluster 2 contains several cancer-related genes that have been implicated in tumor suppression. *AZGP1* is a type of extracellular matrix and secreted glycoprotein. It is a TSG for breast, prostate, and pancreatic cancers, as well as other malignant tumors[30]. *MSMB* is a predictor of favorable outcomes after prostate cancer surgery[31]. This suggests that their expressions are reduced in high-grade PanNETs. Cluster 3 includes the ubiquitin ligase *DTX1*, which has been reported to be a TSG in head and neck and gastric cancers[32,33]. Its association with pancreatic tumors is unclear, but it may have a tumor-suppressive effect on low-grade PanNETs. Cluster 3 was also highly expressed in one G3 case, indicating the heterogeneity of PanNETs.

This gene expression profiling reinforced the notion that tumors with high Ki-67 have a unique transcriptional landscape potentially linked to oncogenes, which may be especially true for the group with Ki-67 indices of ≥ 10% (G3 and G2-high). The oncogene upregulation in the group with Ki-67 indices of ≥ 10% (G3 and G2-high) suggests a pathway that could be targeted in future therapeutic strategies.

This study has several limitations. First, the study was conducted at a single center, which provided detailed clinicopathological information, and the sample size was especially small for analysis using WES, CCP, and GEP. The limited sample size can be attributed to several factors: the project HOPE study only included cases from 2014 onward; the decision to collect resected specimens was left to the discretion of the attending physicians; and specimens with suspected contamination were excluded. Although there were 62 eligible resected PanNET cases between 2014 and 2022, only 19 were available for analysis. Continued case accumulation and standardized, appropriate sampling are essential moving forward. Second, long-term follow-up is necessary to confirm recurrence and survival due to the good prognosis of the disease; it is often difficult because of comorbidities or the request of the patient to terminate hospital visits. The cause of the loss of the ATRX protein expression in an *ATRX* mutation case with VUS is unknown, but it may be due to an abnormality in the intron region. In the future, whole-genome sequencing should be performed to elucidate this.

In conclusion, our findings advocate for the possibility that the biological grade and molecular profiles including mutations and gene expression in PanNETs may differ around the Ki-67 index cut-off of 10%. This has implications for patient prognosis and treatment strategies. Continued exploration of the genetic and molecular landscape of PanNETs is essential for the development of personalized therapies to optimize the prognosis of patients affected by this complex malignancy.

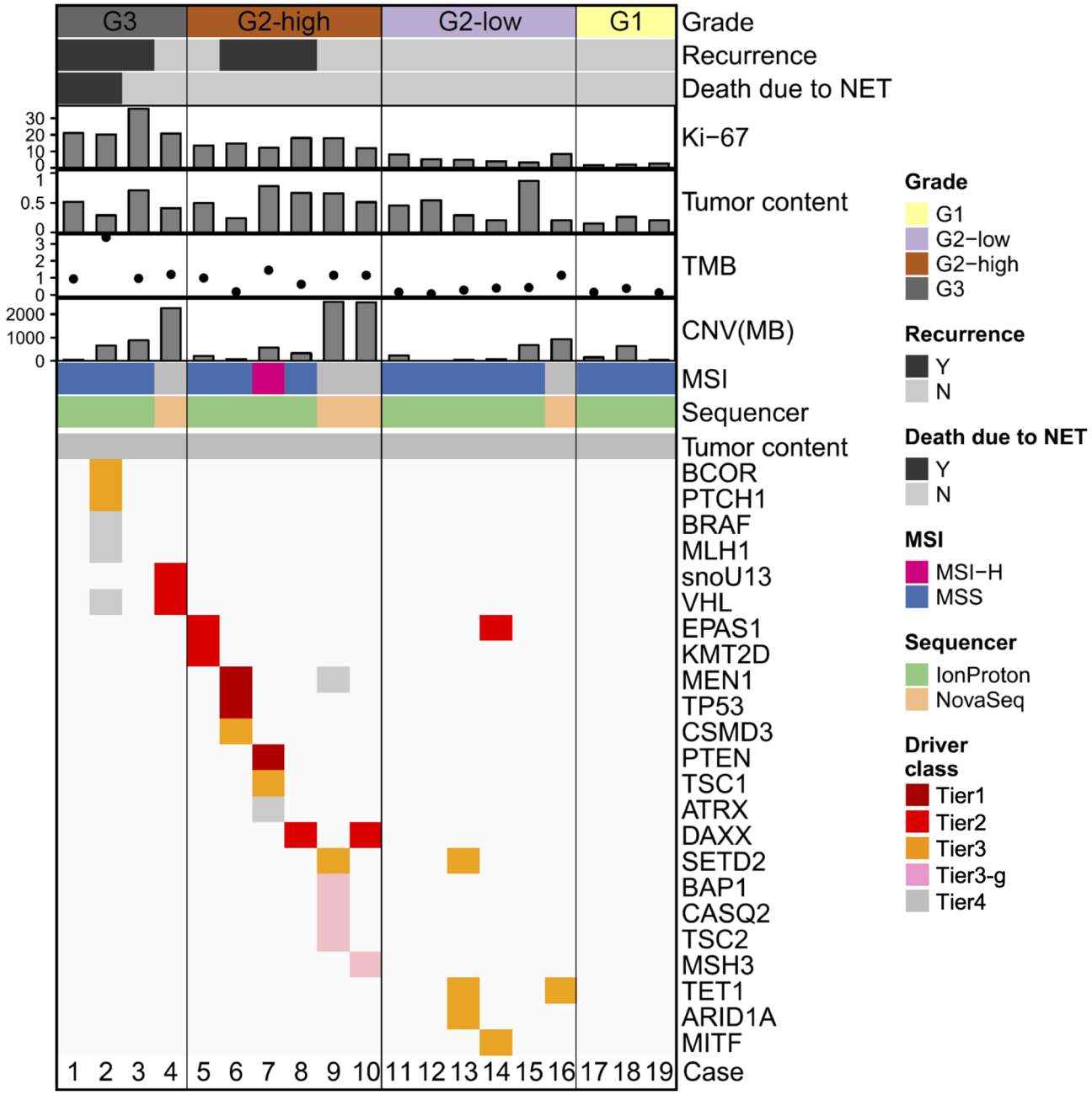

Fig. 3. Oncoprint showing the cancer-related mutations obtained by WES and CCP for 19 cases of pancreatic neuroendocrine tumors (PanNETs). The status of recurrence, mortality, grade, Ki-67, tumor mutation burden (TMB), copy number variants (CNV) size, microsatellite instability (MSI), sequencing method, and purity are shown above the mutation data. Tier 1, driver; Tier 2, likely driver; Tier 3, predicted driver; Tier 3-g, predicted driver (germline); Tier 4, variant of uncertain significance. Tier 4 includes only genes previously reported to be associated with PanNETs.

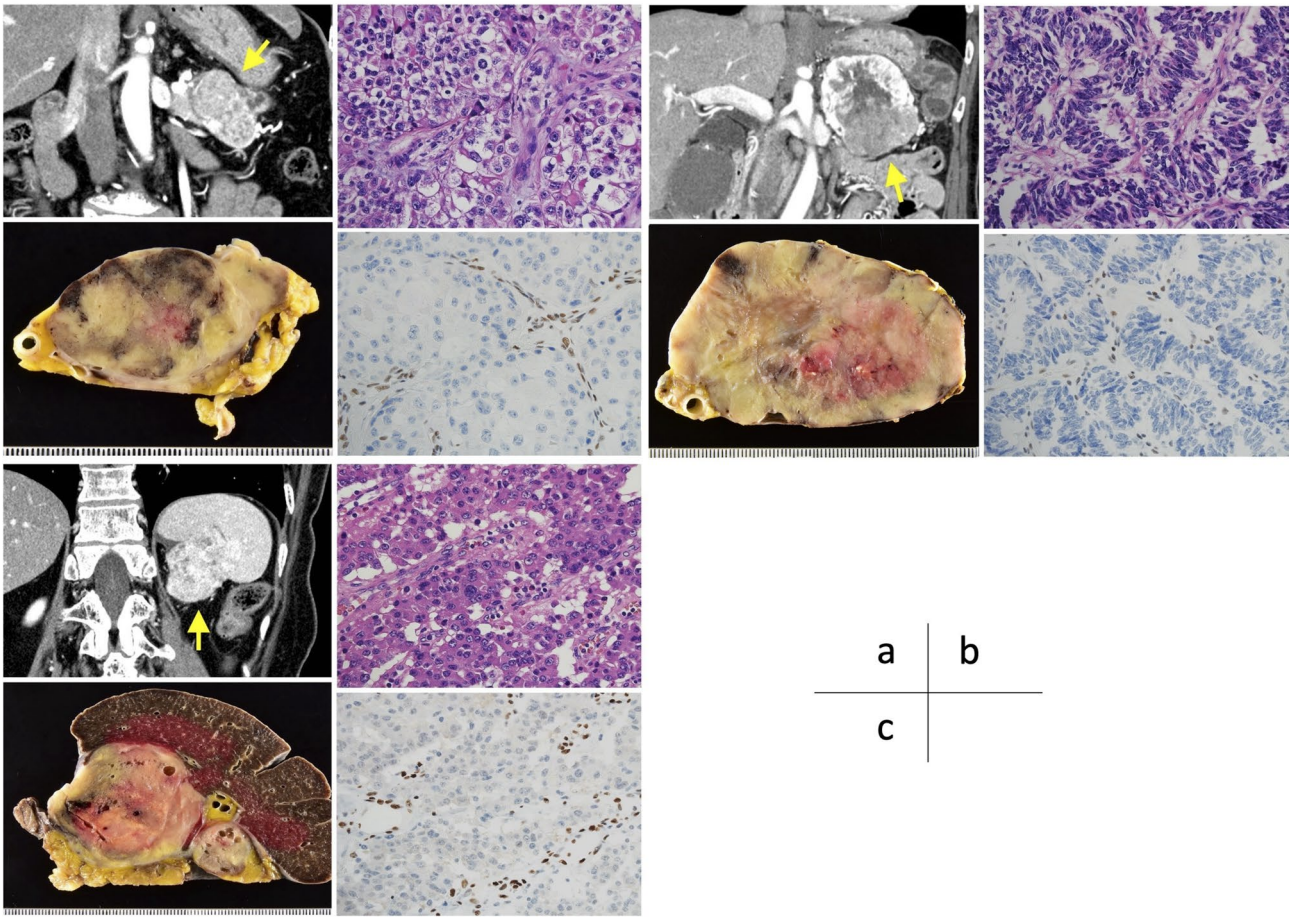

Fig. 4. Immunostaining in 2 cases of truncating mutations of *DAXX* and 1 case of *ATRX* mutation with a variant of uncertain significance. **(a**, **b)** Immunostaining showed loss of DAXX. **(c)** Immunostaining showed loss of ATRX.

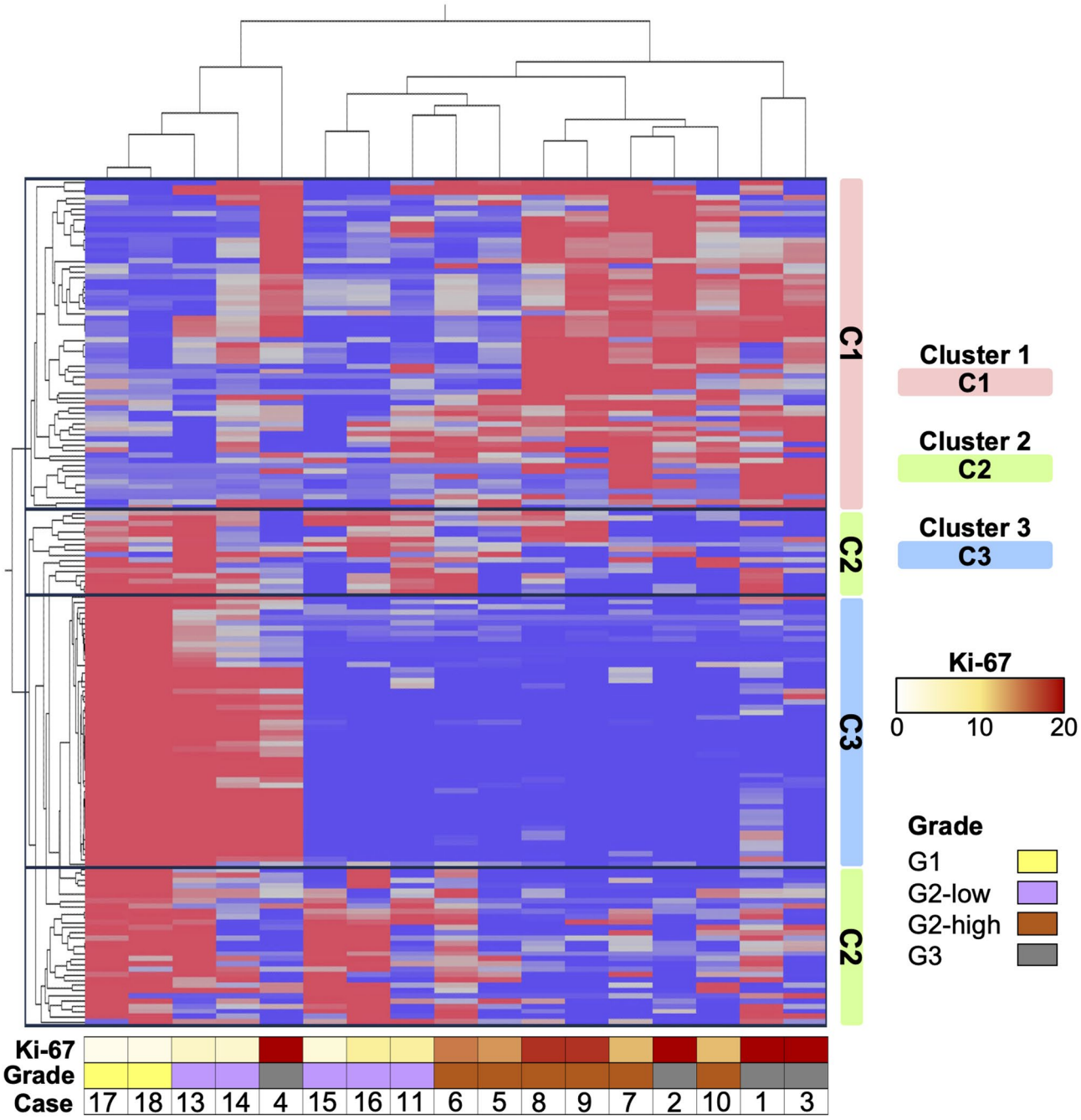

Fig. 5. Heatmap showing hierarchical clustering of differentially expressed genes in 17 PanNETs. **Cluster 1**: upregulation in the group with Ki-67 indices of ≥ 10% and includes 4 oncogenes; **Cluster 2**: upregulation in the groups with Ki-67 indices of < 10%, including 2 oncogenes and 2 tumor suppressor genes; and **Cluster 3**: downregulation mainly in the groups with Ki-67 indices of ≥ 10% and upregulation in some of the groups with Ki-67 indices of < 10%, including a tumor suppressor gene and 7 genes expressed in normal pancreatic islets.

	Oncogene	Tumor suppressor gene	Others		
Cluster 1	*BIRC5* *CDH12* *ELANE* *SERPINA1*		*ACMSD* *AGT* *APOH* *ATF5* *BTBD17* *C9orf24* *CCNB2* *CRNDE* *ENTPD8* *FGA* *FGB* *FGG* *FOLH1* *FST* *FXYD2* *GAGE7*	*GAS2L3* *GC* *GPR64* *HES6* *HIST2H3 A* *HJURP* *IGFBP3* *IRX1* *IRX2* *IRX3* *KCNJ2* *KIF19* *NTNG2* *NUSAP1* *NXPH4* *POSTN*	*RGS1* *SCGB2 A1* *SLC29 A4* *SLC6 A10P* *SLC6 A8* *SMIM6* *SPON2* *TM4SF4* *UBE2 C* *UGT2B10* *UGT2B11* *UGT2B4* *WDR86* *XLOC_014512*
Cluster 2	*ANK1* *FOXQ1*	*AZGP1* *MSMB*	*APOBEC2* *ASCL2* *C8orf47* *CAPN13* *DAPL1* *DDC* *DIRAS3* *DPT* *ELFN2* *FKBP1B* *GCGR* *GHRH* *GSTA5*	*JPH4* *KCNA6* *KCNK17* *LDHD* *MGST1* *MT1G* *MT1H* *MYBPHL* *NEFL* *NEFM* *OGN* *RBP4* *SH2D3 A*	*SLC30 A2* *SLC35D3* *SLC39 A5* *SRRM4* *TAGLN3* *TGFBR3L* *TSPEAR* *WISP2* *XDH* *XLOC_001453* *XLOC_014512*
Cluster 3		*DTX1*	*AMY1 C* *AQP12 A* *AQP8* *BASP1P1* *CCDC69* *CEL** *CELA2 A* *CELA2B* *CELA3 A* *CELA3B* *CLPS** *CPA1** *CPA2** *CPB1*	*CTRB1* *CTRB2* *CTRC* *CTRL* *CUZD1* *GP2* *KLK1* *LGALS2* *LOC101928320* *PDIA2* *PLA2G1B** *PM20D1* *PNLIP** *PNLIPRP1**	*PNLIPRP2** *PRSS1* *PRSS2* *PRSS3* *RBPJL* *REG1 A* *SERPINI2* *SYCN* *TH* *TMED11P* *TMEM52* *TRIM50* *XLOC_011592*

Table 2. Genes in each of the cluster. * Genes related to normal pancreas.

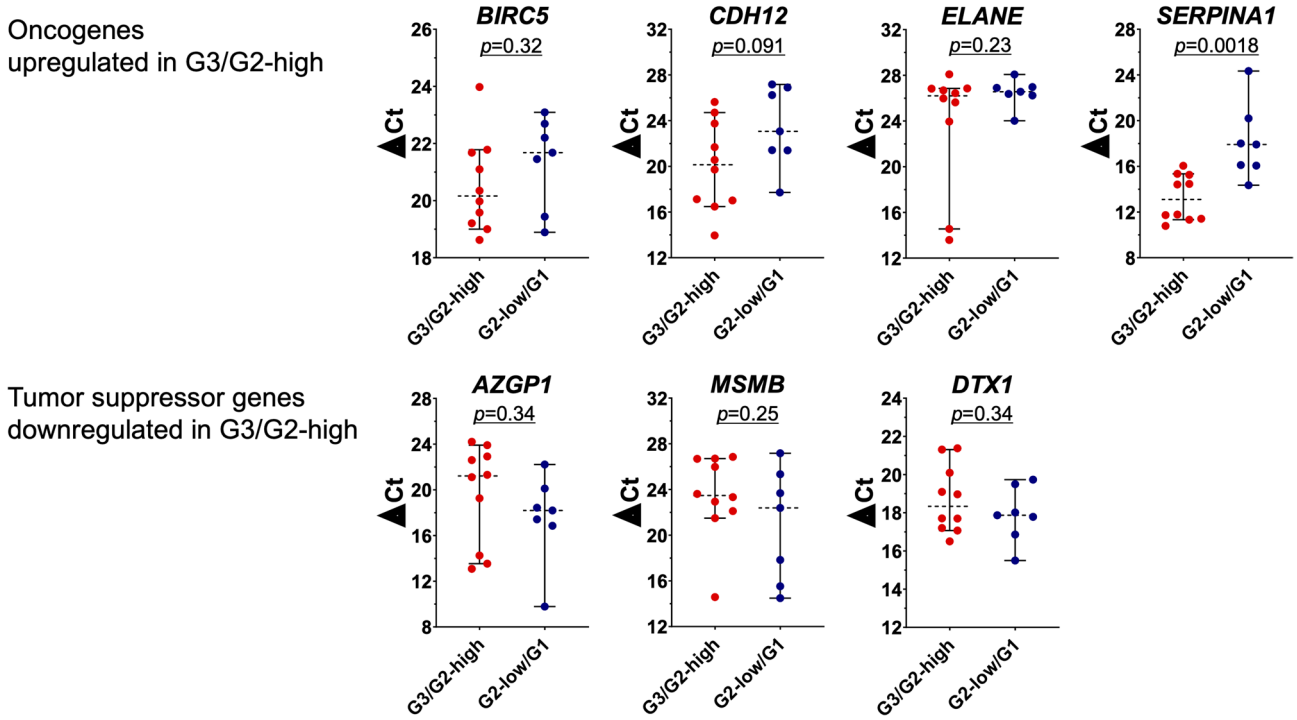

Fig. 6. RT-PCR validation of mRNA expression levels obtained by microarray. Delta Ct values (ΔCt), with lower values indicating higher expression, were shown for 4 oncogenes upregulated in the groups with Ki-67 indices of ≥ 10% (G3 and G2-high, red circles) and 3 tumor suppressor genes downregulated in the groups with Ki-67 indices of < 10% (G2-low and G1, dark blue circles). For samples producing no amplicons after 40 cycles of PCR, the Ct values were considered as 40 to calculate the ΔCt values.

Data availability

In this study, whole exome sequencing and deep sequencing of a comprehensive cancer panel were performed. All data and materials generated during and/or analyzed during this study are available from the corresponding author on reasonable request. Data for this study are confidential patient information regulated by the IRB of the institution. The datasets generated and/or analyzed during the current study are available in the National Bioscience Database Center repository (accession no. hum0127; https://humandbs.biosciencedbc.jp/en/).

Received: 15 December 2024; Accepted: 26 May 2025
Published online: 29 May 2025

References

1. Tang, L. H. et al. Well-differentiated neuroendocrine tumors with a morphologically apparent high-grade component: a pathway distinct from poorly differentiated neuroendocrine carcinomas. *Clin. Cancer Res.* **22**, 1011–1017 (2016).
2. Murakami, M. et al. Machine learning-based model for prediction and feature analysis. *J. Gastroenterol.* **58**, 586–597 (2023).
3. Nuñez-Valdovinos, B. et al. Neuroendocrine tumor heterogeneity adds uncertainty to the world health organization 2010 classification: Real-World data from the Spanish tumor registry (R-GETNE). *Oncologist* **23**, 422–432 (2018).
4. Fujimori, N. et al. Natural history and clinical outcomes of pancreatic neuroendocrine neoplasms based on the WHO 2017 classification; a single-center experience of 30 years. *Pancreatology* **20**, 709–715 (2020).
5. Ricci, C. et al. WHO 2010 classification of pancreatic endocrine tumors. Is the new always better than the old? *Pancreatology* **14**, 539–541 (2014).
6. Pavel, M. et al. Gastroenteropancreatic neuroendocrine neoplasms: ESMO clinical practice guidelines for diagnosis, treatment and follow-up. *Ann. Oncol.* **31**, 844–860 (2020).
7. Nagashima, T. et al. Japanese version of the Cancer genome atlas, JCGA, established using fresh frozen tumors obtained from 5143 cancer patients. *Cancer Sci.* **111**, 687–689 (2020).
8. Kubo, H. et al. Tumor vascularity on contrast-enhanced computed tomography as a predictive marker of metastatic potential for small nonfunctioning pancreatic neuroendocrine tumors. *Surgery* **175**, 484–490 (2024).
9. Thakker, R. V. et al. Clinical practice guidelines for multiple endocrine neoplasia type 1 (MEN1). *J. Clin. Endocrinol. Metab.* **97**, 2990–3011 (2012).
10. Brierley, J. D., Gospodarowicz, M. K. & Wittekind, C. (eds) *TNM Classification of Malignant Tumours* 8th edn (Wiley, 2017).
11. Reid, M. D. et al. Calculation of the Ki67 index in pancreatic neuroendocrine tumors: a comparative analysis of four counting methodologies. *Mod. Pathol.* **28**, 686–694 (2015).
12. Volante, M. et al. Somatostatin receptor type 2A immunohistochemistry in neuroendocrine tumors: a proposal of scoring system correlated with somatostatin receptor scintigraphy. *Mod. Pathol.* **20**, 1172–1182 (2007).
13. Hatakeyama, K. et al. Characterization of tumors with ultralow tumor mutational burden in Japanese cancer patients. *Cancer Sci.* **111**, 3893–3901 (2020).
14. Imamura, T. et al. Genomic landscape of pancreatic cancer in the Japanese version of the Cancer genome atlas. *Ann. Gastroenterol. Surg.* **27**, 491–502 (2022).

15. Ohshima, K. et al. Integrated analysis of gene expression and copy number identified potential cancer driver genes with amplification-dependent overexpression in 1,454 solid tumors. *Sci. Rep.* **7**, 641 (2017).
16. Livak, K. J. & Schmittgen, T. D. Analysis of relative gene expression data using real-time quantitative PCR and the 2(-Delta Delta C(T)) method. *Methods* **25**, 402–408 (2001).
17. Yamaguchi, K. et al. Implementation of individualized medicine for cancer patients by multiomics-based analyses-the project HOPE. *Biomed. Res.* **35**, 407–412 (2014).
18. Jiao, Y. et al. DAXX/ATRX, MEN1, and mTOR pathway genes are frequently altered in pancreatic neuroendocrine tumors. *Science* **331**, 1199–1203 (2011).
19. Scarpa, A. et al. Whole-genome landscape of pancreatic neuroendocrine tumours. *Nature* **543**, 65–71 (2017).
20. Raj, N. et al. Real-time genomic characterization of metastatic pancreatic neuroendocrine tumors has prognostic implications and identifies potential germline actionability. *JCO Precis Oncol* **2**, (2018). PO.17.00267.
21. Hughes, C. M. et al. Menin associates with a trithorax family histone methyltransferase complex and with the hoxc8 locus. *Mol. Cell.* **13**, 587–597 (2004).
22. Marinoni, I. et al. Loss of DAXX and ATRX are associated with chromosome instability and reduced survival of patients with pancreatic neuroendocrine tumors. *Gastroenterology* **146**, 453–460 (2014).
23. Uemura, J. et al. Immunohistochemically detected expression of ATRX, TSC2, and PTEN predicts clinical outcomes in patients with grade 1 and 2 pancreatic neuroendocrine tumors. *Ann. Surg.* **274**, e949–e956 (2021).
24. Yachida, S. et al. Comprehensive genomic profiling of neuroendocrine carcinomas of the Gastrointestinal system. *Cancer Discov.* **12**, 692–711 (2022).
25. Linehan, W. M., Srinivasan, R. & Schmidt, L. S. The genetic basis of kidney cancer: a metabolic disease. *Nat. Rev. Urol.* **7**, 277–285 (2010).
26. Xu, L. et al. BIRC5 is a prognostic biomarker associated with tumor immune cell infiltration. *Sci. Rep.* **11**, 390 (2021).
27. Liu, S. H. et al. BIRC5 is a target for molecular imaging and detection of human pancreatic cancer. *Cancer Lett.* **457**, 10–19 (2019).
28. Ma, J. et al. Cadherin-12 enhances proliferation in colorectal cancer cells and increases progression by promoting EMT. *Tumour Biol.* **37**, 9077–9088 (2016).
29. Kwon, C. H. et al. Snail and serpinA1 promote tumor progression and predict prognosis in colorectal cancer. *Oncotarget* **6**, 20312–20326 (2015).
30. Kong, B. et al. AZGP1 is a tumor suppressor in pancreatic cancer inducing mesenchymal-to-epithelial transdifferentiation by inhibiting TGF-β-mediated ERK signaling. *Oncogene* **29**, 5146–5158 (2010).
31. Dahlman, A. et al. Evaluation of the prognostic significance of MSMB and CRISP3 in prostate cancer using automated image analysis. *Mod. Pathol.* **24**, 708–719 (2011).
32. Hsu, T. S. et al. c-FLIP is a target of the E3 ligase deltex1 in gastric cancer. *Cell. Death Dis.* **9**, 135 (2018).
33. Gaykalova, D. A. et al. Integrative computational analysis of transcriptional and epigenetic alterations implicates DTX1 as a putative tumor suppressor gene in HNSCC. *Oncotarget* **8**, 15349–15363 (2017).

Acknowledgements

We thank Ms. Yuko Watanabe for her technical assistance.

Author contributions

All authors contributed to the study conception and design. Material preparation and data collection and analysis were performed by Y.K., N.O., K.O. and T.N. The first draft of the manuscript was written by Y.K., and all authors commented on previous versions of the manuscript. All authors have read and approved the final manuscript.

Declarations

Competing interests

The authors declare no competing interests.

Additional information

Supplementary Information The online version contains supplementary material available at https://doi.org/10.1038/s41598-025-04356-y.

Correspondence and requests for materials should be addressed to R.A.